### Title

A COX-2/sEH dual inhibitor PTUPB ameliorates cecal ligation and puncture-induced sepsis in mice via anti-inflammation and anti-oxidative stress




### Authors

Zhang, Yan-Feng

Sun, Chen-Chen

Duan, Jia-Xi

et al.



### Publication Date

2020-06-01

### DOI

10.1016/j.biopha.2020.109907

Peer reviewed

HHS Public Access

Author manuscript

*Biomed Pharmacother*. Author manuscript; available in PMC 2022 February 24.

Published in final edited form as:

*Biomed Pharmacother*. 2020 June ; 126: 109907. doi:10.1016/j.biopha.2020.109907.

# A COX-2/sEH dual inhibitor PTUPB ameliorates cecal ligation and puncture-induced sepsis in mice *via* anti-inflammation and anti-oxidative stress

**Yan-Feng Zhang**[1,*], **Chen-Chen Sun**[2,*], **Jia-Xi Duan**[3,4,5], **Hui-Hui Yang**[2], **Chen-Yu Zhang**[2], **Jian-Bing Xiong**[2], **Wen-Jing Zhong**[2], **Cheng Zu**[2], **Xin-Xin Guan**[2], **Hui-Ling Jiang**[2], **Bruce D. Hammock**[6], **Sung Hee Hwang**[6], **Yong Zhou**[2,#], **Cha-Xiang Guan**[2,#]

[1]Department of Cardiovascular Surgery, Xiangya Hospital, Central South University, Changsha, Hunan 410078, China

[2]Department of Physiology, Xiangya School of Medicine, Central South University, Changsha, Hunan 410078, China

[3]Department of Pulmonary and Critical Care Medicine, the Second Xiangya Hospital, Central South University, Changsha, Hunan 410011, China

[4]Research Unit of Respiratory Disease, Central South University, Changsha, Hunan 410011, China

[5]Hunan Diagnosis and Treatment Center of Respiratory Disease, Central South University, Changsha, Hunan 410011, China

[6]Department of Entomology and Nematology and UC Davis Comprehensive Cancer Center, University of California, Davis, CA 95616, USA.

## Abstract

Arachidonic acid can be metabolized to prostaglandins and epoxyeicosatrienoic acids (EETs) by cyclooxygenase-2 (COX-2) and cytochrome P450 (CYP), respectively. While protective EETs are degraded by soluble epoxide hydrolase (sEH) very fast. We have reported that dual inhibition of COX-2 and sEH with specific inhibitor PTUPB shows anti-pulmonary fibrosis and renal protection. However, the effect of PTUPB on cecal ligation and puncture (CLP)-induced sepsis remains unclear. The current study aimed to investigate the protective effects of PTUPB against CLP-induced sepsis in mice and the underlying mechanisms. We found that COX-2 expressions

[#]**To whom correspondence should be addressed:** Prof. Cha-Xiang Guan or Yong Zhou, Department of Physiology, Xiangya Medical School, Central South University, Changsha, Hunan 410078, China, Tel.: +86-731-82355051; Fax: +86-731-82355056, guanchaxiang@csu.edu.cn or zhouyong421@csu.edu.cn.

[*]These authors contribute equally to this work

Author Contributions

CXG and YZ conceived and designed the experiments. CCS, YFZ, JXD, HHY, CYZ, WJZ, and JBX performed the experiments. CCS, YFZ, CZ, XXG, and HLJ analyzed the data. HBD, YZ, and CXG contributed reagents/materials/analysis tools. SHH and BDH designed and synthesized PTUPB. CCS, YFZ, and YZ wrote the paper. CXG, BDH, SHH, and YZ critically reviewed the manuscript.

Conflict of interest

The authors declared no conflict of interest.

Compliance with ethical standards

All animal experiments were approved by the Ethics Committee of the School of Basic Medical Science, Central South University (Changsha, China).

were increased, while CYPs expressions were decreased in the liver, lung, and kidney of mice undergone CLP. PTUPB treatment significantly improved the survival rate, reduced the clinical scores and systemic inflammatory response, alleviated liver and kidney dysfunction, and ameliorated the multiple-organ injury of the mice with sepsis. Besides, PTUPB treatment reduced the expression of hypoxia-inducible factor-1α in the liver, lung, and kidney of septic mice. Importantly, we found that PTUPB treatment suppressed the activation of NLRP3 inflammasome in the liver and lung of septic mice. Meanwhile, we found that PTUPB attenuated the oxidative stress, which contributed to the activation of NLRP3 inflammasome. Altogether, our data, for the first time, demonstrate that dual inhibition of COX-2 and sEH with PTUPB ameliorates the multiple organ dysfunction in septic mice.

**Keywords**

sepsis; dual COX-2 and sEH inhibitor; NLRP3 inflammasome; oxidative stress; multiple organ dysfunction

## 1. Introduction

Sepsis is one of the most disturbing disorders in modern intensive care units (ICU) worldwide [1]. Although it has profound progress in both clinical and basic research, the morbidity and mortality remain high, varying from 15% to 40% depending on the severity [2, 3]. However, the effective treatment of sepsis is limited in supportive care, and there is a lack of approved specific molecular therapies [4].

Sepsis is defined as a life-threatening organ dysfunction caused by a dysregulated host response to infection, which is defined by the Sepsis-3 taskforce [3]. Organ dysfunction is assessed by 2 points or more of the Sequential (Sepsis-related) Organ Failure Assessment (SOFA) score, which is directly associated with prognosis [3]. When microbes invade into the body, pathogen-associated molecular patterns (PAMPs) derived from the component of pathogens and damage-associated molecular patterns (DAMPS) derived from injured tissues are released [5]. The NLRs family pyrin domain containing 3 (NLRP3) inflammasome is activated when PAMPs or DAMPs are recognized through pattern recognition receptors (PRRs) [6]. Subsequently, NLRP3 forms an inflammasome complex, cleaves procaspase-1 into the active caspase-1 form, results in the maturation and secretion of pro-inflammatory cytokines such as IL-1β and IL-18, and then aggravates inflammatory response [7]. Recently, NLRP3 inflammasome is the key mediator in mediating inflammatory responses after sepsis [8, 9]. The expression of TLR4, NLRP3, and caspase-1 proteins were significantly increased in tissues after CLP, accompanied by the increase of proinflammatory cytokines in the plasma [8]. Inhibiting NLRP3 inflammasome activation attenuates myocardial dysfunction in mice with sepsis [8, 10]. Considering the lack of effective therapies in sepsis, it may be a potential therapeutic target to suppress the NLRP3 inflammasome activation.

The metabolites of arachidonic acid (ARA) play a vital role in inflammation [11]. In inflammatory conditions, ARA is released from membrane phospholipids by the enzyme phospholipase A2 (PLA2) and metabolized by cyclooxygenases (COXs), lipoxygenases

(LOXs), and cytochrome P450s (CYPs) to prostaglandins (PGs)/thromboxane, leukotrienes, and epoxy-/hydroxy-metabolites such as epoxyeicosatrienoic acids (EETs) and other EpFA, respectively [12]. Among them, COX-2 metabolites are involved in inflammatory disorders [13]. A massive release of PGs and leukotrienes induced by bacterial flagellin results in the rapid death of mice [14]. On the contrary, four distinct EET regioisomers, namely 5,6-, 8,9-, 11,12- and 14,15-EET, have been identified with anti-inflammation, cardio-protection, and organ protection effects [15, 16]. However, EETs and the other EpFA have very short half-lives. They are readily metabolized by soluble epoxide hydrolase (sEH) to dihydroxyeicosatrienoic acids (DHETs) with no or less bioactivity [17]. In our previous studies, inhibition of sEH activity alleviated acute lung injury (ALI) induced by lipopolysaccharide (LPS) through suppressing the expression of triggering receptor expressed on myeloid cells-1 (TREM-1) [18, 19]. However, it remains unknown whether the metabolic pattern of ARA changes during sepsis and subsequently inhibiting both COX and sEH pathways of ARA protect against sepsis.

Cumulatively, these studies indicate that inhibition of either COX-2 or sEH is beneficial for inflammation and cardiovascular disease. Recently, we have synthesized a dual COX-2 and sEH inhibitor, 4-(5-phenyl-3-{3-[3-(4-trifluoromethyl-phenyl)-ureido]-propyl}S-pyrazol-1-yl) benzenesulfonamide (PTUPB), which has anti-tumor, anti-fibrosis, and renal protection [16, 20–22]. More interestingly, the effect of PTUPB on inhibiting tumor growth and metastasis is more prominent compared with inhibitors that are selective on either pathway, either as a single agent or in a combination [16]. In this study, we hypothesized that concurrently inhibiting COX-2 and sEH by PTUPB would be efficacious in attenuating sepsis. Here, we demonstrated that PTUPB promoted the survival of septic mice by alleviating multiple-organ dysfunction.

## 2. Materials and Methods

### 2.1 Animals

Adult male C57BL/6 mice (20 ± 2 g) were purchased from Hunan SJA Laboratory Animal Co., Ltd (Hunan, China). The animals were housed in a specific pathogen-free environment, given free access to water and food, and exposed to a 12-h light/dark cycle. Mice were handled in accordance with the guidelines of the National Institutes of Health. All animal experiments were approved by the Ethics Committee of the School of Basic Medical Science, Central South University (No.2019-LW003, Changsha, China).

### 2.2 Establishment of sepsis model induced by cecal ligation and puncture (CLP)

Mice were randomly divided into the following groups (40 mice per group): the sham group, CLP group, and CLP + PTUPB group. CLP was performed according to a previous report [23]. Briefly, the mice were anesthetized with 1% pentobarbital sodium (80 mg/kg) by intraperitoneal injection, and then the abdomen was carefully shaved and cleaned with complex iodine. Next, a 0.5–1 cm longitudinal midline incision was made at the lower abdomen with a sterilized blade. The cecum was isolated and exteriorized out of the abdominal cavity gently. The cecum was ligated at the midpoint with a 4–0 silk suture with the strength of the blood supply obstructed. Next, a puncture was performed in a

through-and-through pattern puncture midway using used a 22G needle between the ligation and the tip of the cecum from mesenteric to antimesenteric side, avoiding vascular injury. After removing the needle, a small droplet of feces was extruded from both penetration holes, followed by relocating the cecum into the abdominal cavity. The abdominal cavity and incision were closed. Pre-warmed sterile saline (37 °C, 5 mL/100 g body weight) was injected subcutaneously for resuscitation. The whole operation was carried out on a sterilized board. Mid-grade sepsis was initiated with this procedure. For the sham group, the cecum was relocated into the abdominal cavity without ligation and puncture. PTUPB (5 mg/kg) or the corresponding solvent polyethylene glycol 400 (PEG 400) [22] was subcutaneously administered 72, 48, and 24 h before CLP for CLP + PTUPB group and CLP group respectively. Finally, the mice were returned to their cages with free access to food and water. After 24 h, the mice were sacrificed, and portions of tissues were immediately snap-frozen in liquid nitrogen and then stored at −80 °C for analysis.

### 2.3 Clinical score

Twenty-four hours after the CLP, a clinical score was used to evaluate the presence and severity of sepsis [24], based on the following six symptoms or signs: periorbital exudates, lethargy, diarrhea, tremors, labored respiration, and piloerection. Each measure was scored 1. The total scores of each mouse were collected for the analysis.

### 2.4 Liver and kidney function tests

Twenty-four hours after the CLP, blood samples were isolated by eyeball extirpation followed by centrifugation with 3000 revolutions per minute (rpm) for 10 min. Then, the serum was isolated for liver and kidney function tests with the automatic biochemical analyzer (Hitachi automatic biochemical analyzer 7000, Japan), including blood urea nitrogen (BUN), creatine (Cre), serum alanine aminotransferase (ALT), aspartate aminotransferase (AST), lactate dehydrogenase (LDH), albumin (ALB), and total protein (TP).

### 2.5 Measurement of the percentage of neutrophils

To measure the percentage of neutrophils, Wright’s stain was performed. The dyes of basic methylene blue and acid eosin were used. Neutrophils were discriminated based on the characteristics of different cells. First, 20 μL anticoagulated blood was placed on and spread over a glass slide thinly with the edge of another slide to produce a monolayer of cells. The prepared blood smear was then air-dried completely. Liquid A (Polysciences, Germany) was placed on the film, and liquid B (Polysciences, Germany) was added 1 min later. The slide was washed with distilled water after 10 min-staining and was air-dried thoroughly. One hundred leukocytes were counted under an oil microscope (Olympus, Japan), and then neutrophils were differentiated to calculate the percentage. Besides, the myeloperoxidase (MPO) activity in liver, lung, and kidney tissues was measured according to the manufacturer’s instruction (Jiancheng Bioengineering Institute, Nanjing, China).

### 2.6 Enzyme-linked immunosorbent assay (ELISA)

The protein level of monocyte chemoattractant protein-1 (MCP-1) in serum was measured using an ELISA kit (Invitrogen, Thermo Fisher Scientific, Cat: BMS6005TEN USA) according to the manufacturer's instructions. The concentrations of the MCP-1 were quantified by reference to a standard curve.

### 2.7 Hematoxylin-eosin (H&E) staining and organ injury score

H&E staining was performed as described in our previous study [25]. The left lung, liver median lobe, and the left kidney were isolated for histopathological analysis. After fixation in 4% paraformaldehyde overnight, samples were embedded in paraffin and sectioned in 3 μm thick slices. After dehydration with a graded series, the slices were stained with hematoxylin and eosin. The liver injury score was measured according to the damage of hepatic lobular structure as follows: intact-1, intact with cell swelling-2, mild disruption-3, marked disruption-4. Lung injury score was measured according to five independent variables: hemorrhage, proteinaceous debris filling the airspace, neutrophils in the alveolar space, hyaline membranes, and septal thickening. A score of 0 represented no damage; l, <25% damage; 2, 25 to 50% damage; 3, 50 to 75% damage and 4, > 75% damage. Kidney injury score was measured according to the percentage of damaged tubules to the total number of tubules as follows: 1, <25% damage; 2, 25 to 50% damage; 3, 50 to 75% damage; 4, 75 to 90% damage and 5, >90% damage. The score of 3 fields per slide was calculated, respectively. All scoring was performed by four pathologists in a blinded manner.

### 2.8 Total RNA extraction and real-time PCR

Mouse liver, lung, and kidney tissues were homogenized in Trizol solution (Takara, Japan) for RNA extraction according to the manufacturer's protocol. The cDNA was generated by reverse transcription from RNA (1 μg) based on the Reverse Transcription System kit (Takara, Japan). Real-time PCR was implemented using SYBR Green (Takara, Japan) on the Bio-Rad real-time PCR system (CFX96 Touch™, Bio-Rad, USA). The primers of genes for need detected and housekeeping gene β-actin were synthesized by Invitrogen. Primer sequences used in this study are shown in Table 1. According to our previous study [22, 26], the relative gene expression was measured by the $2^{-\Delta\Delta CT}$ methods. The profile of CYPs was calculated using the $2^{-\Delta CT}$ method.

### 2.9 Western Blot

Total protein extraction and western blot were performed according to our previous study [27]. Briefly, mouse liver, lung, and kidney tissues were homogenized and lysed in cold RIPA buffer (Solarbio, cat: R0010 Beijing, China), which contained a protease inhibitor (Roche, Mannheim, cat: P0100 Germany). The protein concentration determined with Pierce™ BCA Protein Assay Kit (Thermo Fisher Scientific cat: 23229). The proteins were mixed with loading buffer and denatured at 100 °C for10 mins. Then the lysates were separated using an SDS-PAGE gel, and the proteins were transferred onto 0.45-μm polyvinylidene difluoride (PVDF) membranes. The membranes were blocked with 5% fat-free milk and were incubated overnight at 4°C with rabbit anti-COX-2 antibody (1:2000, Servicebio, cat: GB111037, Wuhan, China), goat anti-pro-IL-1β antibody (1:2000,

R&D, cat: AF-401-NA, USA), rabbit anti-NLRP3 antibody (1:2000, CST, cat: #15101, USA), mouse anti-HIF-1α antibody (1:2000, Immunoway, cat: sc-13515, China), rabbit anti-β-actin antibody (1:7500, Signalway, cat: #21338, China), rabbit anti-GAPDH antibody (1:2000, Servicebio, cat: GB11002, Wuhan, China), rabbit anti-β-tubulin antibody (1:2000, Servicebio cat: GB13017-2). Subsequently, the membranes were washed three times with TBST and were incubated for 1 h at room temperature with anti-rabbit (COX-2, NLRP3, β-actin, β-tubulin, and GAPDH, Signalway, cat: #L3012-2), anti-goat (pro-IL-1β, absin, cat: abs20005ss) or anti-mouse (HIF-1α, Signalway, cat: L3032-2) horseradish peroxidase-conjugated secondary antibodies. The proteins were detected with a gel imaging system (Bio-Rad, Hercules, CA). The expression of proteins in the liver, lung, and kidney was respectively normalized to β-tubulin, β-actin, or GAPDH as a loading control.

### 2.10 Measurement of superoxide dismutase (SOD) and malondialdehyde (MDA)

The SOD activity and contents of MDA in liver, lung, and kidney tissues were measured according to their respective kits following the manufacturer's instructions (Jiancheng Bioengineering Institute, Cat: A001-1-2, Cat: A003-4-1, Nanjing, China).

### 2.11 Statistical analysis

Statistical analysis was processed by SPSS 22.0 (IBM, Chicago, IL) or GraphPad Prism 7.0 software (San Diego, CA, USA). Unpaired *t*-tests were used to compare the means of two groups. One-way ANOVA was used for comparison among the different groups. *Tukey's* test was used as a post hoc test to make pair-wise comparisons. *P*-value < 0.05 was considered statistically significant.

## 3. Results

### 3.1 COX-2/CYP pathway of ARA metabolism dysregulation occurs during sepsis

Firstly, we studied the profile of ARA metabolism by COX-2 and CYP during CLP-induced sepsis. In mice, CYP2J5, CYP2J6, CYP2J9, CYP2C44, and CYP2C29 are in response to the synthesis of EETs. We found CYP2J5 was the most abundant in the liver, CYP2J6/2J9 in the lung, and CYP2J5 in the kidney (Figure 1A–1C). While all of those enzymes were downregulated during CLP-induced sepsis (Figure 1D–1F). In contrast, the protein of COX-2 was upregulated in the liver, lung, and kidney by CLP (Figure 1G–1J). These results indicate a dysregulation of CYP/COX-2 pathways of ARA metabolism in mice with sepsis.

### 3.2 PTUPB improves the survival rate and health status of septic mice

After confirming that PTUPB had no deleterious effect on the liver, lung, and kidney morphology in healthy mice, we tested PTUPB in the CLP-induced sepsis mice. We found that the survival rate in the CLP+PTUPB group was higher than that in the CLP mice (40% vs. 15%) (Figure 2A). To further assess the health status of living mice, the clinical scores of the mice in the three groups were investigated 24 h after the surgery. The clinical score of survivors in the CLP+PTUPB group was 2.50 ± 1.96, which was significantly lower than that in the CLP group (4.44 ± 1.24) (Figure 2B). These results demonstrate that PTUPB increases survival and improves the health status of septic mice.

### 3.3 PTUPB improves the liver and kidney functions in septic mice

Clinically, blood BUN and Cre are the two main biomarkers of kidney function, while high levels of serum ALT, AST, and LDH reveal liver function disorders. Our data demonstrated that the levels of BUN and creatine in the CLP group were significantly higher than those in the sham group, which were significantly decreased by PTUPB treatment (Figure 3A–3B). We also found that CLP increased serum ALT, AST, and LDH (Figure 3C–3E), but decreased ALB and TP levels (Figure 3F–3G), which were partially reversed by PTUPB (Figure 3C–3G). These results indicate that PTUPB improves the liver and kidney function in septic mice.

### 3.4 PTUPB attenuates the injury of multiple organs in septic mice

Furthermore, we investigated the effects of PTUPB on tissue injury induced by sepsis using H&E staining and organ injury scores. We found that CLP-induced remarkable injuries in liver, lung, and kidney tissue, which were characterized by structure disorder of hepatic lobular, diffuse vacuolation of hepatocyte (Figure 4A), significant thickening of the alveolar walls, the collapse of the alveolar (Figure 4C), glomerular structure disorder, the tubular cell swelling and infiltration of inflammatory cells (Figure 4E), respectively. These pathological changes were all alleviated by PTUPB pretreatment, which was confirmed by the corresponding tissue injury score (Figure 4). These results indicate that PTUPB attenuates multiple tissue injuries in septic mice.

### 3.5 PTUPB reduces the systemic inflammatory response in septic mice

Sepsis is characterized by the activation of innate immune cells, an increase of pro-inflammatory cytokines, and chemokines. Here, we examined the percentage of neutrophils in the blood, MPO activity, and the expression of TNF-α and MCP-1. We found that PTUPB treatment decreased the percentage of neutrophils and MPO activity in the liver, lung, and kidney (Figure 5A–5B). Levels of MCP-1 in serum (Figure 5C), as well as mRNA of *Mcp-1* and *Tnf-α* in the liver, lung, and kidney (Figure 5D–5E), were also suppressed by PTUPB treatment. These data indicate that PTUPB reduces the systemic inflammatory response in septic mice.

### 3.6 PTUPB inhibits the NLRP3 inflammasome activation in septic mice

The NLRP3 inflammasome is an intracellular multiprotein complex that mainly controls the maturation and release of IL-1β family [28]. IL-1β is one of the inflammatory cytokines that contribute to the development of sepsis [29]. We found that PTUPB reduced the protein expression of both NLRP3 and pro-IL-1β in the liver, lung, and kidney induced by CLP (Figure 6A–6F). These results indicate that PTUPB inhibits the NLRP3 inflammasome activation in septic mice.

### 3.7 PTUPB attenuates oxidative stress in septic mice

Multiple organ dysfunction secondary to sepsis is associated with a surge of pro-oxidants and reduced antioxidant activity. MDA is one of the end products of lipid peroxidation, which was increased in the liver, lung, and kidney of mice with sepsis, while PTUPB reduced the MDA content in the lung and kidney, rather than in the liver (Figure 7A).

The activity of SOD, an antioxidant, was not changed in the liver by sepsis. The activity of SOD in the lung was decreased, whereas it was increased in the kidney by sepsis. PTUPB treatment promoted the SOD activity in both lung and kidney compared with CLP (Figure 7B). We further observed that PTUPB significantly increased the mRNA of *heme oxygenase-1* (*Ho-1*) (Figure 7C). These results indicate that PTUPB attenuates oxidative stress in septic mice.

### 3.8 PTUPB suppresses the expression of HIF-1α in septic mice

Hypoxia-inducible factor-1α (HIF-1α) exerts a significant role in the regulation of hypoxic stress and inflammation. Results showed that PTUPB reduced the HIF-1α protein and mRNA expression in the liver, lung, and kidney of the CLP-treated mice (Figure 8A–8E).

## 4. Discussion

We previously reported that an sEH inhibitor attenuated LPS-induced ALI and bleomycin-induced pulmonary fibrosis [18, 19, 30]. Further, the results of our present study illustrated that ARA metabolic pathways were dysregulated in sepsis, which is characterized by an increase of COX-2 and reduction of CYPs. Thus, it is a reasonable therapeutic strategy to restore the balance of ARA metabolism by inhibiting COX-2 activity and increasing the level of EETs via sEH inhibition. Thus, we employed a COX-2 and sEH dual inhibitor PTUPB in CLP-induced sepsis in mice. We found that PTUPB improved the survival and partially reversed multiple organs (the lung, kidney, and liver) injuries in septic mice. The protective role of PTUPB may be mediated by inhibiting the NLRP3 inflammasome activation and expression of pro-inflammatory cytokines, as well as increasing SOD activity and stimulating the HIF-1α pathway.

ARA was first found in the 1970s, and it can be metabolized by COXs, LOXs, and CYPs. Bitto et al. demonstrated that a dual inhibitor of COX-2 and 5-LOX protected mice from sepsis induced by CLP through inhibiting the inflammatory response [31]. Here, our study indicated that restoring the imbalance of COX/CYP pathways may be a potential therapeutic approach. It has been known that COX-2 metabolites, as well as EETs and other EpFA, participate in many inflammatory disorders [13, 32]. EI-Achakar et al. reported that the expression of COX-2 was TLR4-dependent in sepsis [33]. After binding with TLR4 on the membrane of macrophages, LPS activates the MyD88-TAK1-NF-κB/MAPK signaling cascades and TRIF pathway, associated with the upregulation of expression of COX-2 [34, 35]. Some studies suggest that COX-2 inhibition attenuates sepsis and sepsis-related organ dysfunction [36, 37]. However, there is also contrary evidence. For example, COX-2 protects against early onset of gut origin sepsis through promoting enterocyte migration and decreasing epithelial permeability of the ileum [38, 39]. Our results suggested that the regulation of both the COX-2 and CYP pathways of ARA attenuated multiple-organ dysfunction and mortality of septic mice. Particularly in the CLP model, an inflammatory response is needed to control bacterial infection. The results here illustrate the earlier hypothesis of Schmeltzer's work that the downregulation of COX-2 and other enzymes by EETs resulted more in encouraging the resolution of inflammation than in blocking inflammation [40].

It has long been recognized that infections cause damage not only because of the virulence of the microorganisms but also the host response [41]. The local infection will extend to the entire body mainly through the circulation of innate immune cells and inflammatory cytokines with auto-amplified activation property, which is called “cytokines storm” [42]. Among the cytokines, IL-1β production is critically regulated by NLRP3 inflammasomes [43]. NLRP3 inflammasomes consist of NLRP3 proteins, adapter protein apoptosis-associated speck-like protein (ASC), and procaspase-1 [44]. When PAMPs released by pathogens or DAMPs released by damage host cells bind to PRRs expressed in innate immune cells, the NLRP3, ASC, and pro-caspase-1 were assembled into a complex. Then activated caspase-1 promotes the secretion of IL-1β and IL-18, resulting in the excessive inflammatory response [45]. Increasing evidence demonstrate that CYP-derived epoxylipids, such as EETs, exhibit anti-inflammatory properties [18, 46, 47]. Our previous study has shown that sEH inhibition, approaching to elevate the levels of these lipid mediators, can attenuate LPS-induced ALI in mice by suppressing inflammation [18]. Genetic deletion of sEH protects against myocardial injury by inhibiting the activation of NLRP3 inflammasome [47]. In the present study, we found that dual inhibition of COX-2/sEH by PTUPB significantly inhibited CLP-induced NLRP3 and pro-IL-1β expression in mice with sepsis. The above results indicated that PTUPB could inhibit the activation of NLRP3 inflammasome.

Excessive pro-inflammatory cytokines and mitochondrial dysfunction induce oxidative stress, which is characterized by an imbalance between antioxidant defense effectiveness and the speed of ROS generation, causing a net overload oxidants [48]. ROS attack proteins and membrane lipids to produce harmful intermediary molecules such as MDA and the 4-hydroxy-2-nonenal (4-HNE). Another study also indicates that ROS promotes NLRP3 activation [49]. SOD is considered to be a potent antioxidant that catalyzes the dismutation of the superoxide anion into hydrogen peroxide ($H_2O_2$). Here, we found that COX-2/sEH dual inhibitor PTUPB reduced the MDA content and increased SOD activity in mice with sepsis. Moreover, HO-1 is strongly up-regulated to protect cells from oxidative injury and inflammatory responses [50]. Numerous studies have demonstrated that HO-1 is up-regulated in sepsis [51, 52]. In cigarette smoke-induced lung injury, EETs have been found to increase the expression of HO-1 [53]. As expected, we found that PTUPB significantly increased the mRNA of *HO-1.* According to our study, we speculated that PTUPB could protect against sepsis by resolving the cytokine storm and oxidative stress.

There are also some limitations to our study. First, we did not measure whether the LOX pathway of ARA metabolism changes after PTUPB treatment. In our other study, while we found that the level of LOX remained constant in the lung after LPS challenged (results were not presented here). Though Jun Yang et al. found that sEH inhibitor decreased LOX metabolites in asthma mice [54], the changes of LOX pathways remain to be determined in sepsis. Secondly, the levels of PGs and EETs after PTUPB administration were not assessed directly. We previously found that PTUPB inhibited COX-2 derived PGF2α, PGD2, and PGJ2. What’s more, the levels of 12,13-DiHOME on the sEH pathway in PDX BL0269 tumor tissues were also decreased [16], suggesting that PTUPB can effectively inhibit the COX-2 and sEH in pathological conditions. This will be done along with the monitoring of oxylipins in later studies with more animals. Moreover, there is a lack of experiments

in vitro in our study. Though we have demonstrated that pro-inflammatory cytokines were dramatically suppressed by PTUPB in inflammatory macrophages [55], the more detailed mechanisms should be elucidated in future studies.

In conclusion, the present study suggests that inhibiting COX-2 and sEH of ARA metabolism by PTUPB would be efficacious in attenuating sepsis through resolving the cytokine storm and oxidative stress. Therefore, we demonstrate here targeting the ARA metabolic disorders may be a promising therapeutic approach to sepsis.

## Funding information

This study was supported by the National Natural Science Foundation of China (No. 81670014, 91949110), Hunan Provincial Natural Science Foundation of China (2018JJ3701, 2019JJ70008), High School Innovation Fund of Hunan province (12K004, 18K009), and Fundamental Research Funds for the Central Universities of Central South University (2019zzts720). Partial support was provided by R35 ES030443 and P42 ES004619 from NIEHS.

## Data Availability

The data used to support the findings of this study are available from the corresponding author upon request.

## References

[1]. Hattori Y, Hattori K, Suzuki T, Matsuda N, Recent advances in the pathophysiology and molecular basis of sepsis-associated organ dysfunction: Novel therapeutic implications and challenges, Pharmacology & therapeutics 177 (2017) 56–66. [PubMed: 28232275]

[2]. Lelubre C, Vincent JL, Mechanisms and treatment of organ failure in sepsis, Nature reviews. Nephrology 14(7) (2018) 417–427. [PubMed: 29691495]

[3]. Singer M, Deutschman CS, Seymour CW, Shankar-Hari M, Annane D, Bauer M, Bellomo R, Bernard GR, Chiche JD, Coopersmith CM, Hotchkiss RS, Levy MM, Marshall JC, Martin GS, Opal SM, Rubenfeld GD, van der Poll T, Vincent JL, Angus DC, The Third International Consensus Definitions for Sepsis and Septic Shock (Sepsis-3), Jama 315(8) (2016) 801–10. [PubMed: 26903338]

[4]. Gotts JE, Matthay MA, Sepsis: pathophysiology and clinical management, BMJ (Clinical research ed.) 353 (2016) i1585.

[5]. van der Poll T, van de Veerdonk FL, Scicluna BP, Netea MG, The immunopathology of sepsis and potential therapeutic targets, Nat Rev Immunol 17(7) (2017) 407–420. [PubMed: 28436424]

[6]. Wu J, Liu B, Mao W, Feng S, Yao Y, Bai F, Shen Y, Guleng A, Jirigala B, Cao J, Prostaglandin E2 Regulates Activation of Mouse Peritoneal Macrophages by Staphylococcus aureus through Toll-Like Receptor 2, Toll-Like Receptor 4, and NLRP3 Inflammasome Signaling, J Innate Immun (2019) 1–16.

[7]. Lempriere S, NLRP3 inflammasome activation implicated in tau pathology, Nat Rev Neurol (2019).

[8]. Yang L, Zhang H, Chen P, Sulfur dioxide attenuates sepsis-induced cardiac dysfunction via inhibition of NLRP3 inflammasome activation in rats, Nitric oxide : biology and chemistry 81 (2018) 11–20. [PubMed: 30273666]

[9]. Rahim I, Djerdjouri B, Sayed RK, Fernandez-Ortiz M, Fernandez-Gil B, Hidalgo-Gutierrez A, Lopez LC, Escames G, Reiter RJ, Acuna-Castroviejo D, Melatonin administration to wild-type mice and nontreated NLRP3 mutant mice share similar inhibition of the inflammatory response during sepsis, J Pineal Res 63(1) (2017).

[10]. Zhang W, Tao A, Lan T, Cepinskas G, Kao R, Martin CM, Rui T, Carbon monoxide releasing molecule-3 improves myocardial function in mice with sepsis by inhibiting NLRP3

inflammasome activation in cardiac fibroblasts, Basic Res Cardiol 112(2) (2017) 16. [PubMed: 28168403]

[11]. Dalli J, Colas RA, Quintana C, Barragan-Bradford D, Hurwitz S, Levy BD, Choi AM, Serhan CN, Baron RM, Human Sepsis Eicosanoid and Proresolving Lipid Mediator Temporal Profiles: Correlations With Survival and Clinical Outcomes, Critical care medicine 45(1) (2017) 58–68. [PubMed: 27632672]

[12]. Schunck WH, Konkel A, Fischer R, Weylandt KH, Therapeutic potential of omega-3 fatty acid-derived epoxyeicosanoids in cardiovascular and inflammatory diseases, Pharmacology & therapeutics 183 (2018) 177–204. [PubMed: 29080699]

[13]. Pereira-Leite C, Nunes C, Jamal SK, Cuccovia IM, Reis S, Nonsteroidal Anti-Inflammatory Therapy: A Journey Toward Safety, Med Res Rev 37(4) (2017) 802–859. [PubMed: 28005273]

[14]. von Moltke J, Trinidad NJ, Moayeri M, Kintzer AF, Wang SB, van Rooijen N, Brown CR, Krantz BA, Leppla SH, Gronert K, Vance RE, Rapid induction of inflammatory lipid mediators by the inflammasome in vivo, Nature 490(7418) (2012) 107–11. [PubMed: 22902502]

[15]. Larsen BT, Campbell WB, Gutterman DD, Beyond vasodilatation: non-vasomotor roles of epoxyeicosatrienoic acids in the cardiovascular system, Trends in pharmacological sciences 28(1) (2007) 32–8. [PubMed: 17150260]

[16]. Gu J, Luo L, Wang Q, Yan S, Lin J, Li D, Cao B, Mei H, Ying B, Bin L, Smith FG, Jin SW, Maresin 1 attenuates mitochondrial dysfunction through the ALX/cAMP/ROS pathway in the cecal ligation and puncture mouse model and sepsis patients, Laboratory investigation; a journal of technical methods and pathology 98(6) (2018) 715–733. [PubMed: 29467458]

[17]. Davis CM, Liu X, Alkayed NJ, Cytochrome P450 eicosanoids in cerebrovascular function and disease, Pharmacology & therapeutics 179 (2017) 31–46. [PubMed: 28527918]

[18]. Zhou Y, Liu T, Duan JX, Li P, Sun GY, Liu YP, Zhang J, Dong L, Lee KSS, Hammock BD, Jiang JX, Guan CX, Soluble Epoxide Hydrolase Inhibitor Attenuates Lipopolysaccharide-Induced Acute Lung Injury and Improves Survival in Mice, Shock 47(5) (2017) 638–645. [PubMed: 27753791]

[19]. Dong L, Zhou Y, Zhu ZQ, Liu T, Duan JX, Zhang J, Li P, Hammcok BD, Guan CX, Soluble Epoxide Hydrolase Inhibitor Suppresses the Expression of Triggering Receptor Expressed on Myeloid Cells-1 by Inhibiting NF-kB Activation in Murine Macrophage, Inflammation 40(1) (2017) 13–20. [PubMed: 27696333]

[20]. Li J, Zhou Y, Wang H, Gao Y, Li L, Hwang SH, Ji X, Hammock BD, COX-2/sEH dual inhibitor PTUPB suppresses glioblastoma growth by targeting epidermal growth factor receptor and hyaluronan mediated motility receptor, Oncotarget 8(50) (2017) 87353–87363. [PubMed: 29152086]

[21]. Hye Khan MA, Hwang SH, Sharma A, Corbett JA, Hammock BD, Imig JD, A dual COX-2/sEH inhibitor improves the metabolic profile and reduces kidney injury in Zucker diabetic fatty rat, Prostaglandins & other lipid mediators 125 (2016) 40–7. [PubMed: 27432695]

[22]. Zhang CY, Duan JX, Yang HH, Sun CC, Zhong WJ, Tao JH, Guan XX, Jiang HL, Hammock BD, Hwang SH, Zhou Y, Guan CX, COX-2/sEH dual inhibitor PTUPB alleviates bleomycin-induced pulmonary fibrosis in mice via inhibiting senescence, FEBS J (2019).

[23]. Rittirsch D, Huber-Lang MS, Flierl MA, Ward PA, Immunodesign of experimental sepsis by cecal ligation and puncture, Nature protocols 4(1) (2009) 31–6. [PubMed: 19131954]

[24]. Alves-Filho JC, Sonego F, Souto FO, Freitas A, Verri WA Jr., Auxiliadora-Martins M, Basile-Filho A, McKenzie AN, Xu D, Cunha FQ, Liew FY, Interleukin-33 attenuates sepsis by enhancing neutrophil influx to the site of infection, Nat Med 16(6) (2010) 708–12. [PubMed: 20473304]

[25]. Zhang YF, Zhang J, Sun CC, Tang CY, Sun GY, Luo WJ, Zhou Y, Guan CX, Vasoactive intestinal peptide inhibits the activation of murine fibroblasts and expression of interleukin 17 receptor C, Cell Biol Int 43(7) (2019) 770–780. [PubMed: 31026365]

[26]. Zhong WJ, Yang HH, Guan XX, Xiong JB, Sun CC, Zhang CY, Luo XQ, Zhang YF, Zhang J, Duan JX, Zhou Y, Guan CX, Inhibition of glycolysis alleviates lipopolysaccharide-induced acute lung injury in a mouse model, J Cell Physiol 234(4) (2019) 4641–4654. [PubMed: 30256406]

[27]. Sun GY, Yang HH, Guan XX, Zhong WJ, Liu YP, Du MY, Luo XQ, Zhou Y, Guan CX, Vasoactive intestinal peptide overexpression mediated by lentivirus attenuates lipopolysaccharide-induced acute lung injury in mice by inhibiting inflammation, Mol Immunol 97 (2018) 8–15. [PubMed: 29544087]

[28]. Martinez-Garcia JJ, Martinez-Banaclocha H, Angosto-Bazarra D, de Torre-Minguela C, Baroja-Mazo A, Alarcon-Vila C, Martinez-Alarcon L, Amores-Iniesta J, Martin-Sanchez F, Ercole GA, Martinez CM, Gonzalez-Lisorge A, Fernandez-Pacheco J, Martinez-Gil P, Adriouch S, Koch-Nolte F, Lujan J, Acosta-Villegas F, Parrilla P, Garcia-Palenciano C, Pelegrin P, P2X7 receptor induces mitochondrial failure in monocytes and compromises NLRP3 inflammasome activation during sepsis, Nat Commun 10(1) (2019) 2711.

[29]. Ge Y, Huang M, Yao YM, Recent advances in the biology of IL-1 family cytokines and their potential roles in development of sepsis, Cytokine Growth Factor Rev 45 (2019) 24–34. [PubMed: 30587411]

[30]. Zhou Y, Yang J, Sun GY, Liu T, Duan JX, Zhou HF, Lee KS, Hammock BD, Fang X, Jiang JX, Guan CX, Soluble epoxide hydrolase inhibitor 1-trifluoromethoxyphenyl-3- (1-propionylpiperidin-4-yl) urea attenuates bleomycin-induced pulmonary fibrosis in mice, Cell Tissue Res 363(2) (2016) 399–409. [PubMed: 26310139]

[31]. Bitto A, Minutoli L, David A, Irrera N, Rinaldi M, Venuti FS, Squadrito F, Altavilla D, Flavocoxid, a dual inhibitor of COX-2 and 5-LOX of natural origin, attenuates the inflammatory response and protects mice from sepsis, Crit Care 16(1) (2012) R32. [PubMed: 22356547]

[32]. Dong R, Hu D, Yang Y, Chen Z, Fu M, Wang DW, Xu X, Tu L, EETs reduces LPS-induced hyperpermeability by targeting GRP78 mediated Src activation and subsequent Rho/ROCK signaling pathway, Oncotarget 8(31) (2017) 50958–50971. [PubMed: 28881620]

[33]. El-Achkar TM, Plotkin Z, Marcic B, Dagher PC, Sepsis induces an increase in thick ascending limb Cox-2 that is TLR4 dependent, Am J Physiol Renal Physiol 293(4) (2007) F1187–96. [PubMed: 17634395]

[34]. McKenna S, Eckman M, Parker A, Bok R, Hurt KJ, Wright CJ, Perinatal Endotoxemia Induces Sustained Hepatic COX-2 Expression through an NFkappaB-Dependent Mechanism, J Innate Immun 8(4) (2016) 386–99. [PubMed: 27160391]

[35]. Chen WC, Tseng CK, Chen YH, Lin CK, Hsu SH, Wang SN, Lee JC, HCV NS5A Up-Regulates COX-2 Expression via IL-8-Mediated Activation of the ERK/JNK MAPK Pathway, PLoS One 10(7) (2015) e0133264. [PubMed: 26231035]

[36]. Sun LC, Zhang HB, Gu CD, Guo SD, Li G, Lian R, Yao Y, Zhang GQ, Protective effect of acacetin on sepsis-induced acute lung injury via its anti-inflammatory and antioxidative activity, Arch Pharm Res 41(12) (2018) 1199–1210. [PubMed: 29243040]

[37]. Ozer EK, Goktas MT, Kilinc I, Bariskaner H, Ugurluoglu C, Iskit AB, Celecoxib administration reduced mortality, mesenteric hypoperfusion, aortic dysfunction and multiple organ injury in septic rats, Biomedicine & pharmacotherapy = Biomedecine & pharmacotherapie 86 (2017) 583–589. [PubMed: 28024294]

[38]. Golden JM, Escobar OH, Nguyen MVL, Mallicote MU, Kavarian P, Frey MR, Gayer CP, Ursodeoxycholic acid protects against intestinal barrier breakdown by promoting enterocyte migration via EGFR- and COX-2-dependent mechanisms, Am J Physiol Gastrointest Liver Physiol 315(2) (2018) G259–G271. [PubMed: 29672156]

[39]. Fredenburgh LE, Velandia MM, Ma J, Olszak T, Cernadas M, Englert JA, Chung SW, Liu X, Begay C, Padera RF, Blumberg RS, Walsh SR, Baron RM, Perrella MA, Cyclooxygenase-2 deficiency leads to intestinal barrier dysfunction and increased mortality during polymicrobial sepsis, J Immunol 187(10) (2011) 5255–67. [PubMed: 21967897]

[40]. Schmelzer KR, Inceoglu B, Kubala L, Kim IH, Jinks SL, Eiserich JP, Hammock BD, Enhancement of antinociception by coadministration of nonsteroidal anti-inflammatory drugs and soluble epoxide hydrolase inhibitors, Proceedings of the National Academy of Sciences of the United States of America 103(37) (2006) 13646–51. [PubMed: 16950874]

[41]. Goh C, Knight JC, Enhanced understanding of the host-pathogen interaction in sepsis: new opportunities for omic approaches, Lancet Respir Med 5(3) (2017) 212–223. [PubMed: 28266329]

[42]. Chousterman BG, Swirski FK, Weber GF, Cytokine storm and sepsis disease pathogenesis, Semin Immunopathol 39(5) (2017) 517–528. [PubMed: 28555385]

[43]. Lv Z, Wang Y, Liu YJ, Mao YF, Dong WW, Ding ZN, Meng GX, Jiang L, Zhu XY, NLRP3 Inflammasome Activation Contributes to Mechanical Stretch-Induced Endothelial-Mesenchymal Transition and Pulmonary Fibrosis, Critical care medicine 46(1) (2018) e49–e58. [PubMed: 29088003]

[44]. Shao BZ, Xu ZQ, Han BZ, Su DF, Liu C, NLRP3 inflammasome and its inhibitors: a review, Front Pharmacol 6 (2015) 262. [PubMed: 26594174]

[45]. Rabeony H, Pohin M, Vasseur P, Petit-Paris I, Jegou JF, Favot L, Frouin E, Boutet MA, Blanchard F, Togbe D, Ryffel B, Bernard FX, Lecron JC, Morel F, IMQ-induced skin inflammation in mice is dependent on IL-1R1 and MyD88 signaling but independent of the NLRP3 inflammasome, Eur J Immunol 45(10) (2015) 2847–57. [PubMed: 26147228]

[46]. Darwesh AM, Jamieson KL, Wang C, Samokhvalov V, Seubert JM, Cardioprotective effects of CYP-derived epoxy metabolites of docosahexaenoic acid involve limiting NLRP3 inflammasome activation (1), Can J Physiol Pharmacol 97(6) (2019) 544–556. [PubMed: 30326194]

[47]. Darwesh AM, Keshavarz-Bahaghighat H, Jamieson KL, Seubert JM, Genetic Deletion or Pharmacological Inhibition of Soluble Epoxide Hydrolase Ameliorates Cardiac Ischemia/Reperfusion Injury by Attenuating NLRP3 Inflammasome Activation, Int J Mol Sci 20(14) (2019).

[48]. Brigelius-Flohe R, Flohe L, Basic principles and emerging concepts in the redox control of transcription factors, Antioxid Redox Signal 15(8) (2011) 2335–81. [PubMed: 21194351]

[49]. Wenzel P, Kossmann S, Munzel T, Daiber A, Redox regulation of cardiovascular inflammation - Immunomodulatory function of mitochondrial and Nox-derived reactive oxygen and nitrogen species, Free Radic Biol Med 109 (2017) 48–60. [PubMed: 28108279]

[50]. Yong SB, Chung JY, Kim SS, Choi HS, Kim YH, CD64-targeted HO-1 RNA interference enhances chemosensitivity in orthotopic model of acute myeloid leukemia and patient-derived bone marrow cells, Biomaterials (2019) 119651.

[51]. Carchman EH, Rao J, Loughran PA, Rosengart MR, Zuckerbraun BS, Heme oxygenase-1-mediated autophagy protects against hepatocyte cell death and hepatic injury from infection/sepsis in mice, Hepatology 53(6) (2011) 2053–62. [PubMed: 21437926]

[52]. Chen X, Wang Y, Xie X, Chen H, Zhu Q, Ge Z, Wei H, Deng J, Xia Z, Lian Q, Heme Oxygenase-1 Reduces Sepsis-Induced Endoplasmic Reticulum Stress and Acute Lung Injury, Mediators Inflamm 2018 (2018) 9413876. [PubMed: 30013453]

[53]. Yu G, Zeng X, Wang H, Hou Q, Tan C, Xu Q, Wang H, 14,15-epoxyeicosatrienoic Acid suppresses cigarette smoke extract-induced apoptosis in lung epithelial cells by inhibiting endoplasmic reticulum stress, Cell Physiol Biochem 36(2) (2015) 474–86. [PubMed: 25968975]

[54]. Yang J, Bratt J, Franzi L, Liu JY, Zhang G, Zeki AA, Vogel CF, Williams K, Dong H, Lin Y, Hwang SH, Kenyon NJ, Hammock BD, Soluble epoxide hydrolase inhibitor attenuates inflammation and airway hyperresponsiveness in mice, Am J Respir Cell Mol Biol 52(1) (2015) 46–55. [PubMed: 24922186]

[55]. Gartung A, Yang J, Sukhatme VP, Bielenberg DR, Fernandes D, Chang J, Schmidt BA, Hwang SH, Zurakowski D, Huang S, Kieran MW, Hammock BD, Panigrahy D, Suppression of chemotherapy-induced cytokine/lipid mediator surge and ovarian cancer by a dual COX-2/sEH inhibitor, Proceedings of the National Academy of Sciences of the United States of America 116(5) (2019) 1698–1703. [PubMed: 30647111]

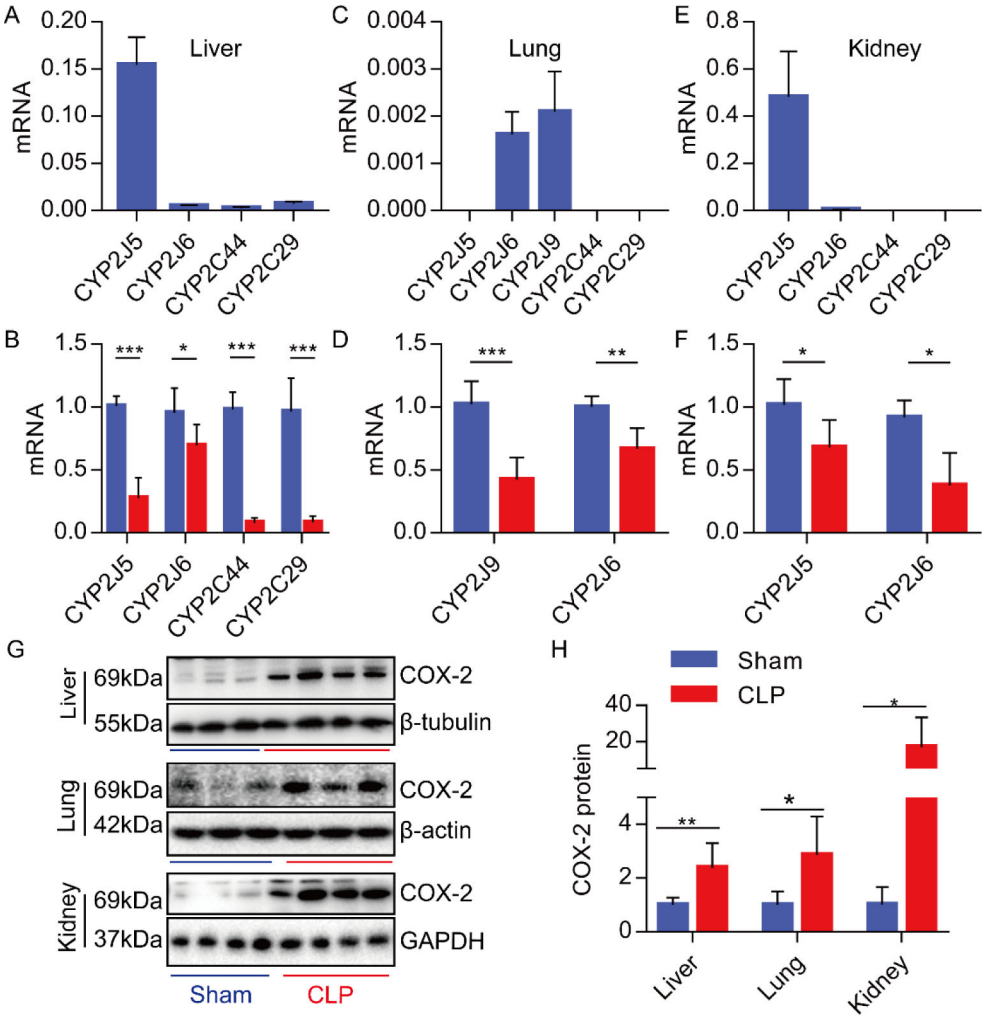


**Figure 1.**

COX-2/CYP pathway of ARA metabolic dysregulation occurs in the liver, lungs, and kidneys during sepsis. CYP2J5 was the most abundant isoform in mouse liver and kidney tissue, while CYP 2J6 and CYP 2J9 were abundant in the lung tissues (the basic expression of CYP isoforms was calculated using the formula $2^{-\Delta CT}$, A-C, $n$=5–7). The *CYP2J5*, *CYP2J6*, *CYP2C44,* and *CYP2C29* mRNA in liver, *CYP2J9,* and *CYP2J6* mRNA in the lung, *CYP2J5* and *CYP2J6* mRNA in kidney were robustly suppressed at 24 h after CLP (the fold change of the CLP group relative to the sham group was calculated using the formula $2^{-\Delta\Delta CT}$, D-F, $n$=5–7). The western blot results manifested that COX-2 protein was increased in the liver, lung, and kidney at 24 h after CLP (representative blots, G-H, $n$=5–8). Data are expressed as the mean ± SD. * $P < 0.05$, ** $P < 0.01$, and *** $P < 0.001$.

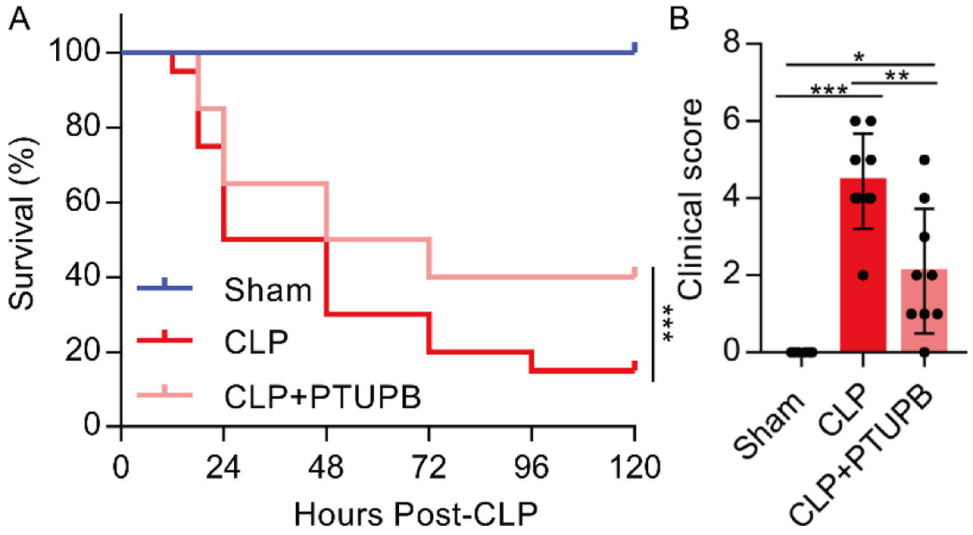


**Figure 2.**

PTUPB improves the survival rate and health status of septic mice. PTUPB (5 mg/kg/day) was administered to mice for 3 consecutive days before CLP, the mortality of the mice was monitored every 6 h, and the percent survival rate was expressed as a Kaplan-Meier survival curve (A, $n$=20 per group). *** $P < 0.001$. Clinical score was used to evaluate the health status of surviving mice (B, $n$=7–9). Data are expressed as the mean ± SD. * $P < 0.05$, ** $P < 0.01$, and *** $P < 0.001$.

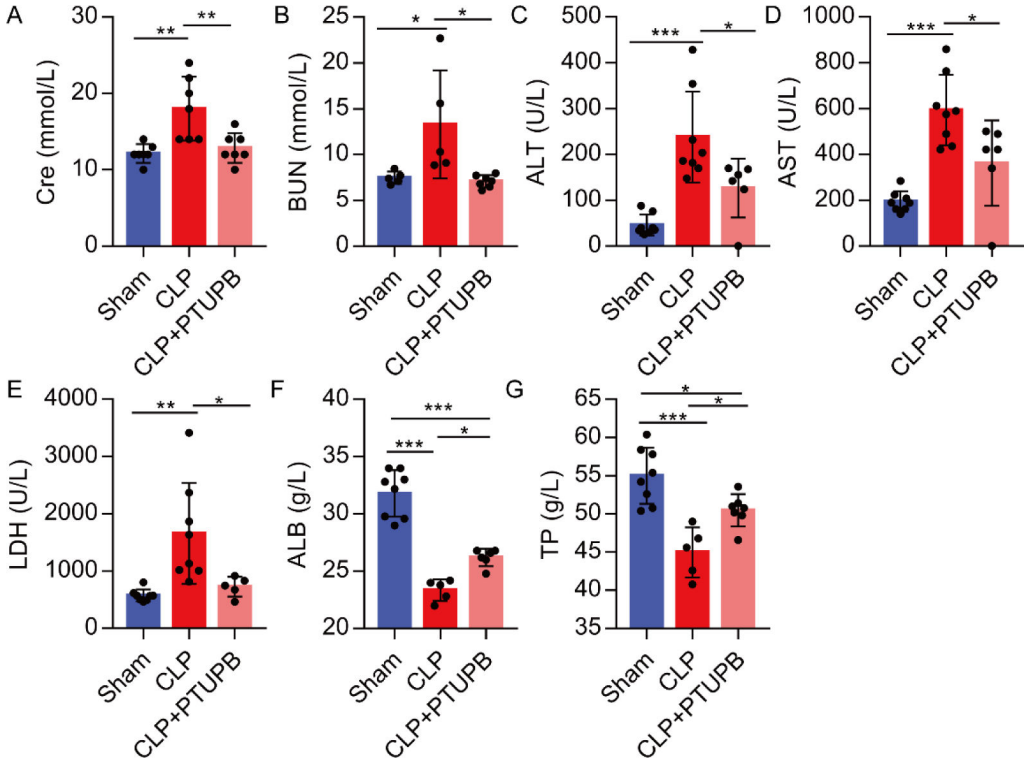


**Figure 3.**

PTUPB improves the liver and kidney dysfunction in septic mice. Levels of serum creatine (Cre) and blood urea nitrogen (BUN), alanine aminotransferase (ALT), aspartate aminotransferase (AST), lactate dehydrogenase (LDH), albumin (ALB) and total protein (TP) were detected (A-G, $n$=5–8). Data are expressed as the mean ± SD. * $P < 0.05$, ** $P < 0.01$, and *** $P < 0.001$.

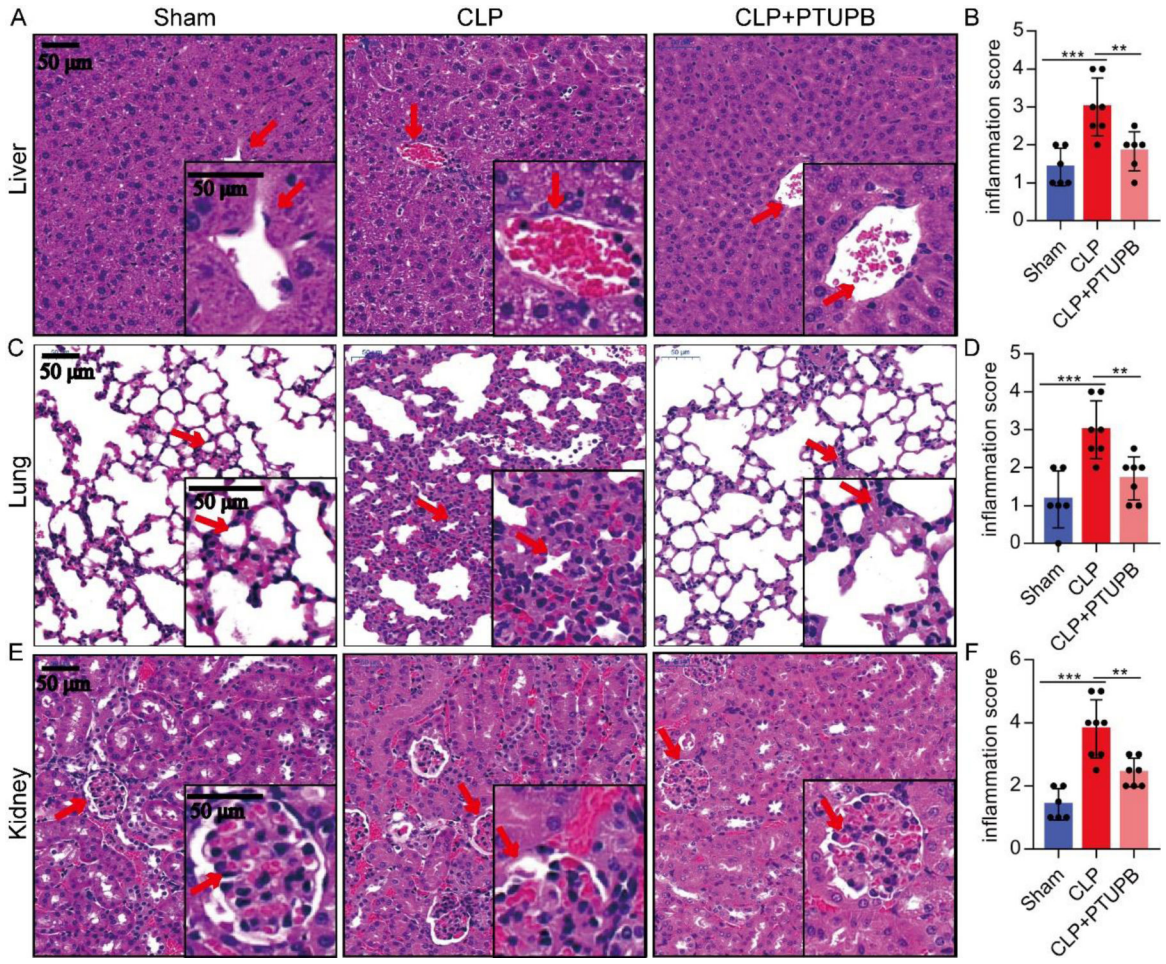


**Figure 4.**

PTUPB attenuates tissue injuries of the liver, lung, and kidney in septic mice. Twenty-four hours after CLP, liver, lung, and kidney tissue histopathology of the mouse was stained with H&E in C57BL/6 mice (A, C, and E). The inflammation injury score was evaluated by four pathologists in a blinded manner (B, $n = 6–7$), (D, $n = 6–7$), and (F, $n = 6–8$). Data are expressed as the mean ± SD. ** $P < 0.01$ and *** $P < 0.001$.

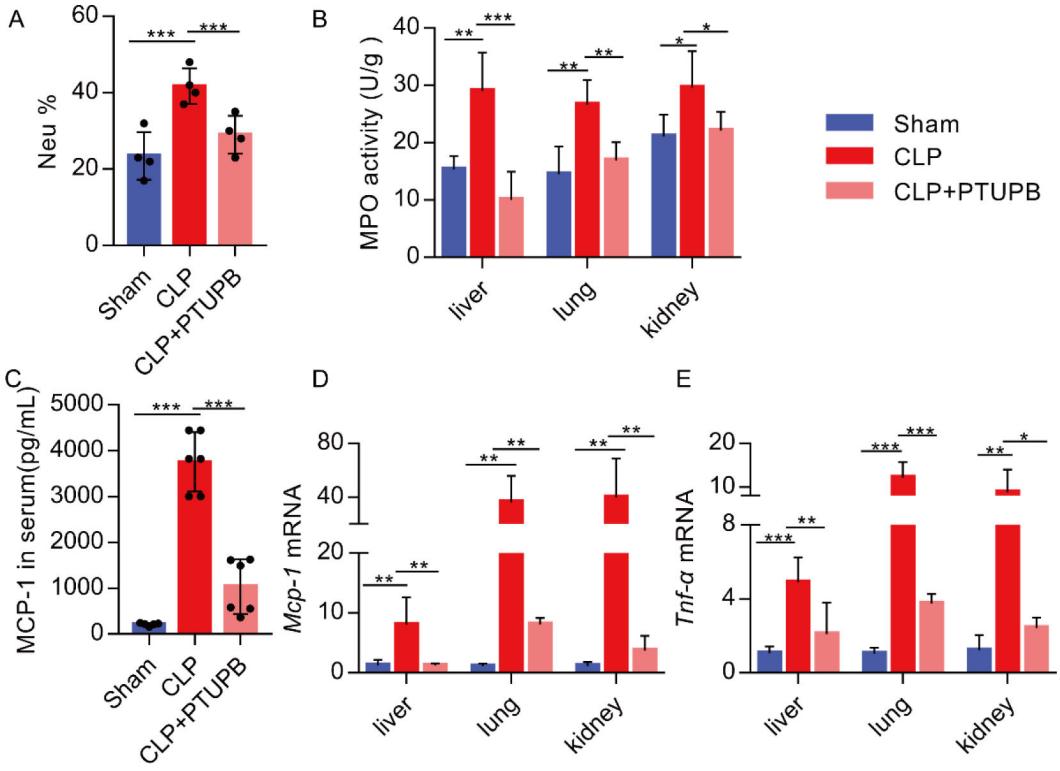


**Figure 5.**

PTUPB reduces the systemic levels of inflammatory factors in septic mice. C57BL/6 mice were subcutaneously injected with PTUPB for three consecutive days before CLP. Twenty-four hours after CLP, the percentage of neutrophils in blood (A, $n$=4). The MPO activity in the liver, lung, and kidney was detected by MPO Kit (B, $n$=5–8). The mRNA expressions of *Mcp-1* and *Tnf-α* in the liver, lung, and kidney were detected by real-time PCR (C, E, $n$=5–7). MCP-1 protein content in serum (D, $n$=6) was detected by an ELISA kit. Data are expressed as the mean ± SD. * $P < 0.05$, ** $P < 0.01$, and *** $P < 0.001$.

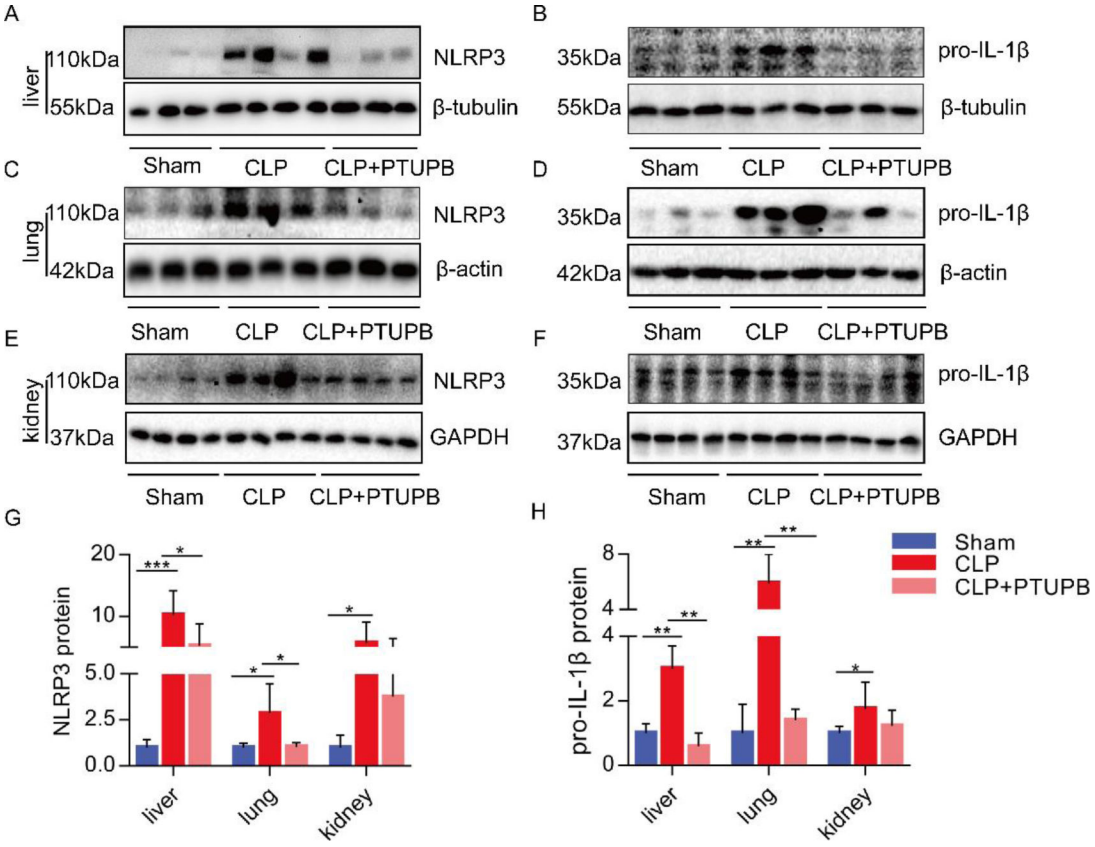


**Figure 6.**

PTUPB inhibits the NLRP3 inflammasome activation in the liver, lung, and kidney of septic mice. The protein expressions of NLRP3 and pro-IL-1β in the liver (representative blots, A-B), lung (representative blots, C-D), and kidney (representative blots, E-F) were detected by western blot ($n$=5–8). G-H: The analysis results of the blot. Data are expressed as the mean ± SD. * $P < 0.05$, ** $P < 0.01$, and *** $P < 0.001$.

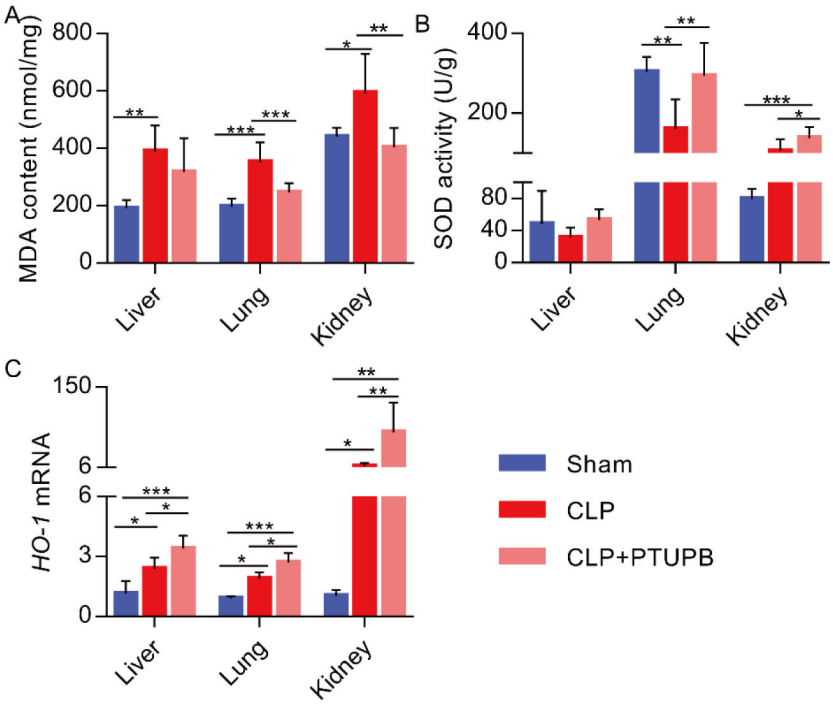


**Figure 7.**

PTUPB decreases oxidative stress of the liver, lung, and kidney in septic mice. C57BL/6 mice were subcutaneously injected with PTUPB for three consecutive days before CLP. The content of MDA and the SOD activity in the liver, lung, and kidney were detected 24 h after CLP (A-B, $n$=5–9). The mRNA expression of *HO-1* in the liver, lung, and kidney was detected by real-time PCR (C, $n$=5–7). Data are expressed as the mean ± SD. * $P < 0.05$, ** $P < 0.01$, and *** $P < 0.001$.

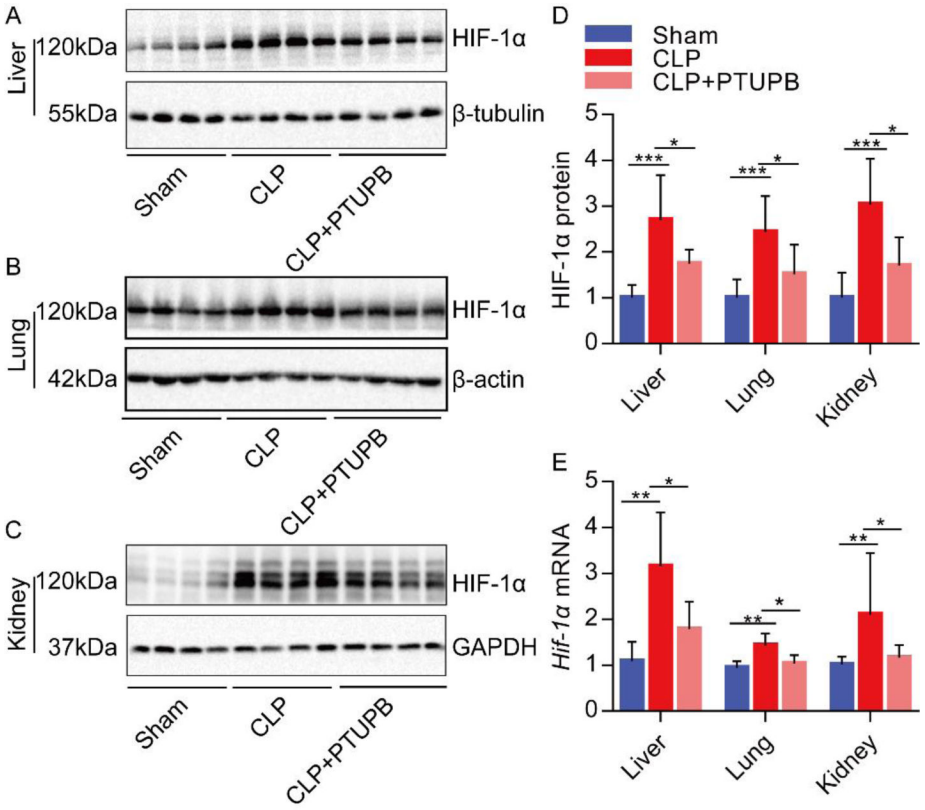


**Figure 8.**

PTUPB suppresses HIF-1α expression in the liver, lung, and kidney of septic mice. The protein expression of HIF-1α in the liver, lung, and kidney was detected by western blot (representative blots, A-D, $n$=5–8). The mRNA expression of *Hif-1α* in the liver, lung, and kidney was detected by real-time PCR (E, sham, $n$=5 CLP, $n$=8, CLP+PTUPB, $n$=7). Data are expressed as the mean ± SD. * $P < 0.05$, ** $P < 0.01$, and *** $P < 0.001$.

**Table 1.**

Primer sequences used to quantitate gene expression in this study

| Gene | Forward primer (5′–3′) | Reverse primer (5′–3′) |
|---|---|---|
| *Cyp2j5* | TGATGGGTTCATCAGCAGGC | CTTGGCTCATCTGGGTTCCAAT |
| *Cyp2j6* | GGTGCCCTTGTTGTTAGCAC | GGCTAACAAGGAGCCGGTAG |
| *Cyp2j9* | AGTCAGTCACCGCCTTTGTG | GTCTCATTGCACGCACTCTC |
| *Cyp2c29* | CCATGGTTGCAGGTAAACCACAT | TCTGTCCCTGCACCAAAGAG |
| *Cyp2c44* | CAAGGTACCCCGAGTGAAGAA | CACGGCATCTGTATAGGGCA |
| *Ho-1* | GTGACAGAAGAGGCTAAGACCG | ACAGGAAGCTGAGAGTGAGGAC |
| *Hif-1α* | CCACCCGCTCTTCTGTCTA | TGGTTTGTGAGTGAGGGT |
| *Mcp-1* | GTCCCTGTCATGCTTCTGG | GCGTTAACTGCATCTGGCT |
| *pro-IL-1β* | CAGGCAGGCAGTATCACTCA | AGCTCATATGGGTCCGACAG |
| *Tnf-α* | AGCCCCCAGTCTGTATCCTT | CTCCCTTTGCAGAACTCAGG |
| *β-actin* | TTCCAGCCTTCCTTCTTG | GGAGCCAGAGCA GTAATC |